Available online at www.sciencedirect.com
ScienceDirect
Optics and Lasers in Engineering 45 (2007) 1107–1114
OPTICS and LASERS in ENGINEERING
www.elsevier.com/locate/optlaseng

# Localization of iris in gray scale images using intensity gradient

A. Basit*, M.Y. Javed

*College of Electrical and Mechanical Engineering, National University of Sciences and Technology (NUST), Peshawar Road, Rawalpindi 46000, Pakistan*

Received 9 May 2007; received in revised form 20 June 2007; accepted 21 June 2007
Available online 23 August 2007

**Abstract**

A new method of iris localization based on intensity value analysis is proposed in this paper. Iris recognition systems are mainly dependent on the performance of iris localization processing. Steps after localization involve normalization, feature extraction and matching. These steps are based on the accuracy and efficiency of localization of iris in human eye images. In the proposed scheme, the inner boundary of iris is calculated by finding the pupil center and radius using two methods. In the first method, selected region is adaptively binarized and centroid of the region utilized for obtaining pupil parameters. Edges are processed to detect radius and center of pupil during the second method. For outer iris boundary, a band is calculated within which iris outer boundary lies. Signals in one dimension are picked up along radial direction within determined band at different angles. Three points with maximum gradient are selected from each signal. Redundant points are deleted using Mahalanobis distance and remaining points are used to obtain the outer circle of the iris. Points for upper and lower eyelids are found in the same way as the iris outer boundary. Selected points are then statistically fitted to make parabolas and lastly eyelashes are removed from the image to completely localize the iris. Experimental results show that proposed method is very efficient and accurate.


*Keywords:* Iris localization; Iris segmentation; Biometrics

## 1. Introduction

People images along with their names are stored automatically in human brain. Whenever a name is thought, the image of the related person comes in mental imagery system. Automatic identification of people is becoming very important [1] particularly after 9/11. Traditionally, two methods *knowledge-based* and *token-based* are used for human identification [2]. Knowledge-based systems are those in which some word/phrase (password) or a number (pin) has to be remembered and in Token-based systems, token (card, key) must be present to prove identity. Both systems are vulnerable: knowledge could be forgotten/shared and token can be stolen/shared. The solution to these problems is identification/verification through biometric. Biometrics is the branch of science in which human beings are automatically identified with their behavioral (signature, gait, voice, etc.) or physical (face, finger, iris, retina, hand geometry, palm print, etc.) characteristics [3–8]. Latest area of research in biometrics is iris recognition that started two decades ago. Iris is the colored part of eye between pupil and sclera. Iris begins to form in the third month of gestation [9,10]. The structures creating its pattern are largely completed by the eighth month although pigment accretion can continue into the first postnatal year. The human iris has unique features and is complex enough to be used as a biometric signature [11] and it never changes during a person's lifetime. The randomness of iris patterns has a very high dimensionality for making recognition decisions reliable with a high level of confidence. Its complex pattern contains many distinctive features such as arching ligaments, furrows, ridges, crypts, rings, corona, freckles and zigzag collarette [4–8]. Iris is neither influenced by external environment nor can it be surgically modified without unacceptable risk to vision [12]. These properties make iris one of the most secure biometric characteristics for identification. Not only the irises of identical twins are different but also left and right irises of the same person are different. The iris consists of a

*Corresponding author. Tel.: +92 333 519 7173.
*E-mail address:* abdulbasit1975@gmail.com (A. Basit).

0143-8166/$ - see front matter © 2007 Elsevier Ltd. All rights reserved.
doi:10.1016/j.optlaseng.2007.06.006

number of layers; the lowest is the epithelium layer, which contains dense pigmentation cells. The stromal layer lies above the epithelium layer and contains blood vessels, pigment cells and the two iris muscles. The density of stromal pigmentation determines the color of the iris. The externally visible surface of the multi-layered iris contains two zones which often differ in color. Outer ciliary and inner pupillary zones are divided by the collarette, which appears as a zigzag pattern [9,13]. Formation of the unique patterns of the iris is random and not related to any genetic factors. The only characteristic that is dependent on genetics is the pigmentation of the iris that determines its color. Due to the epigenetic nature of iris patterns, the two eyes of an individual contain completely independent iris patterns and identical twins possess uncorrelated iris patterns. Human eye images contain sclera, iris, pupil, eyelids, eyelashes and some skin outside the eye. Localization of iris from the other parts of eye in such images is a challenging work which is discussed in this paper.

## 2. Background and related work

Iris is modeled by two circles, one for iris/pupil boundary and other for iris/sclera boundary and two parabolas for upper and lower eyelids [14,15]. This model has been used in several areas including iris recognition, eye tracking and animation [17,18]. In 1993, Daugman [4] built a recognition system and the identification accuracy was up to 100% and localization accuracy was 98.6% using an integro-differential operator to locate the borders of the iris. Wildes [7] system used border detection based on the gradient and Hough transform to locate the iris in the image. Cui [14] used coarse to fine strategy and modified Hough transform. Shen et al. [21] applied wavelet analysis for localization of iris.

Daugman [4] used the following integro-differential operator to localize the iris:

$$\max_{(r,x_0,y_0)} \left| G_\sigma(r)^* \oint_{r,x_0,y_0} \frac{I(x,y)}{2\pi r}\, \mathrm{d}s \right|.$$

In this expression, $I(x, y)$ is an image containing eye. The integro-differential operator searches over the image domain $(x, y)$ for the maximum in the blurred partial derivative with respect to increasing radius $r$ of the normalized contour integral of image along a circular arc "d$s$" of radius "$r$" and center coordinates $(x_0, y_0)$. The symbol * denotes convolution and $G(r)$ is a smoothing function like Gaussian subject to the value of $\sigma$. The complete operator behaves as a circular edge detector, blurred at a scale set by $\sigma$, searching iteratively for the maximal contour integral derivative at successively finer scales of analysis through the three parameter space of center coordinates and radius $(x_0, y_0, r)$ defining a path of contour integration. Daugman did not find the upper and lower eyelids, it simply excluded the upper and lower most portions of the image where eyelid occlusion was expected to occur.

Wildes and Asmuth [6] localized the iris by applying edge detection filter and Hough transform. Edge points were obtained and then circles are fitted to localize the iris [6,7]. Contours for the upper and lower eyelids were fitted in a similar fashion using parameterized parabolic arcs in place of the circle.

Cui et al. [14] decomposed the image using Haar wavelet and localized pupil in coarse to fine strategy. Modified Hough transform followed by a differential operator was used to localize the iris. Lower and upper eyelids were estimated by fitting the parabolic arcs on points obtained using frequency property of the eyelash. Parameters were adjusted to find the true position of the parabolas.

Shen et al. [21] proposed minimum variance method based on wavelet analysis for localizing pupil and used an improved brightness gradient method for iris outer boundary localization.

Iris localization is generally done by combining edge detectors and curve fitting since iris is the annular part between pupil and sclera. The boundaries of the iris are modeled by two non-concentric circles and the eyelids are modeled by two parabolic curves.

In the present paper, an accurate and efficient iris localization method through gray scale intensity value analysis is proposed. Iris localization costs nearly more than half of the total time used till iris code generation and is very important for the subsequent processing such as iris normalization, feature extraction and matching. Therefore, the iris localization is crucial for the performance of the iris recognition system. Iris recognition methods require accurate iris localization for successful processing [16].

## 3. Proposed scheme

For every iris recognition system, accuracy of the iris recognition system is highly dependent on accurate iris localization. The better the iris is localized, the better will be the performance of the system. The proposed scheme of iris localization is composed of four steps as shown in Fig. 1. In first step, iris/pupil boundary (i.e. between pupil and iris) and center of pupil is identified. Two methods for different versions of the database are proposed. Second step involves in finding iris/sclera boundary (i.e. between iris and sclera) and center of the iris. Upper and lower

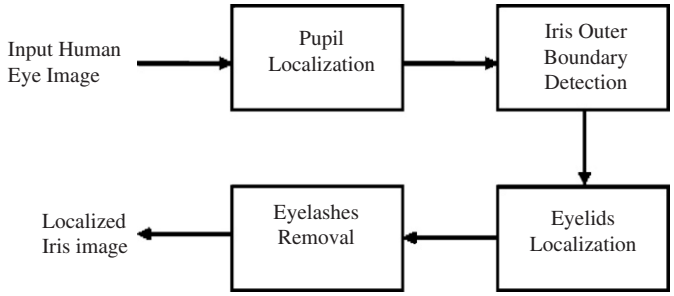


Fig. 1. Layout of iris localization system.

eyelids are estimated in third step and fourth step is used for eyelash removal in order to completely isolate the iris.

### 3.1. Iris/pupil boundary (CASIA Ver 1.0)

In the first step of iris localization, center and radius of pupil is detected. As pupil is smooth and dark portion in the image of eye, moving average filter is applied to the image. For faster processing the border (of width 50 pixels) is not used while calculating moving averages. Following formulas are used to find a point inside the pupil:

$$P_x = \arg\min \sum_{\text{col}} I(x,y),$$

$$P_y = \arg\min \sum_{\text{row}} I(x,y),$$

where $I(x, y)$ is the image portion on which moving average filter is performed. Border width is added to $P_x$ and $P_y$ to get a point $(P_x, P_y)$ which lies inside the pupil. Then, a squared region is selected by taking the point $(P_x, P_y)$ as center. Once a point in the pupil is found, next step is to make binary image by finding adaptive threshold based on maximum value in histogram of the region. Centroid of the region is obtained using the following equations:

$$C_x = \frac{M_x}{A},$$

$$C_y = \frac{M_y}{A},$$

where $M_y = \iint_w x\,\mathrm{d}A$, $M_x = \iint_w y\,\mathrm{d}A$ and $A = \iint_w \mathrm{d}x\,\mathrm{d}y$ where $A$ is the area of window $w$. Centroid of the binary image provides the center of the pupil. Radius of the pupil is calculated by moving in different directions and counting non-zeros in the binary image. Mean of these numbers gives the radius. This method is robust even if eyelashes are present near pupil boundary.

Radius = mean {no. of consecutive non-zeros in different directions from pupil center}.

As exact center is determined, radius of pupil is calculated by finding the average of maximum number of consecutive zeros in four different directions from the center of the pupil. Iris/pupil boundary circle along with its center is shown in Fig. 2(a).

### 3.2. Iris/pupil boundary (CASIA Ver 3.0)

The images in iris database CASIA Ver 3.0 have eight white small circles in the pupil. These small circles are making a round shape. To find the pupil in such images, the following procedure is adopted. A point in pupil is obtained using the same method as discussed in previous section. Edge image is taken and edges with small length are deleted to obtain an image with pupil edge containing no edge inside pupil. As location of a point in pupil is known, horizontal and vertical lines are used to find the first crossing point in left, right, upward and downward directions. Average of first left and first right intersection points on horizontal line from the point in pupil is new $x$-coordinate and average of first upper and lower intersections is new $y$-coordinate of the pupil. This process is iterated till single pixel accuracy is achieved. Lower row of Fig. 2(b) shows iris/pupil boundary and pupil center for images from CASIA Ver 3.0.

### 3.3. Iris/sclera boundary

To reduce the effect of sharp features in determining iris/sclera boundary Gaussian filter of size $27 \times 27$ with standard deviation sigma of value three is applied to the image and filtered image is used for further estimation of the boundary. Different sizes of the filter are experimented. Smaller size does not provide the image with sufficient blurring and larger size filter blend the iris/sclera boundary too much. After that, a band of two circles is calculated with in which iris/sclera boundary is laid. This band is used to reduce the computation time.

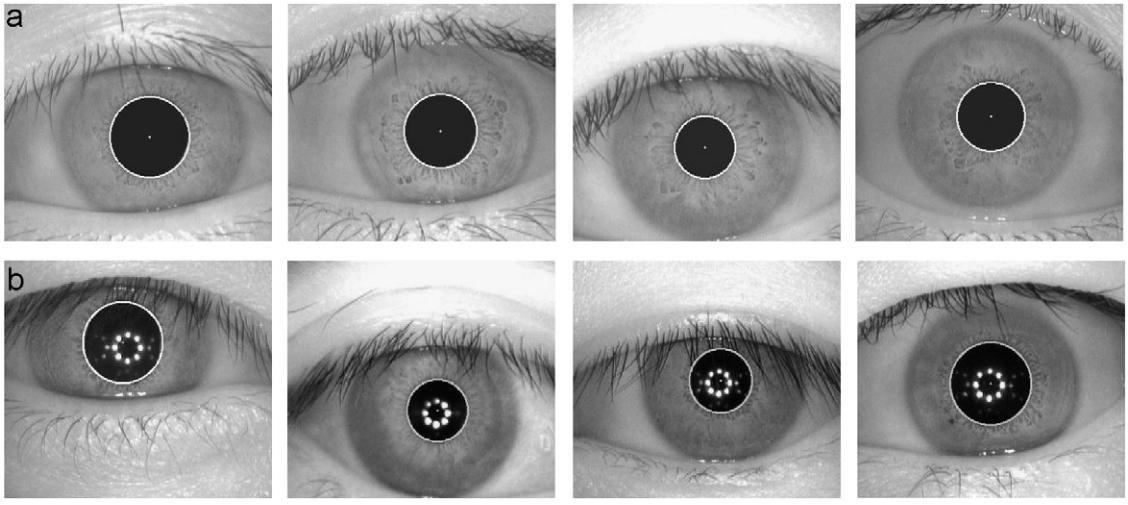


Fig. 2. Iris/pupil boundary with white circle and dot is pupil center: (a) CASIA Ver 1.0 and (b) CASIA Ver 3.0.

The radii of outer and inner circles of the band are based upon the radius of pupil and the distance of first crest along horizontal line passing through the center of pupil in the filtered image, respectively. Graph of horizontal line passing through the center of the pupil displaying first crest and filtered image are shown in Fig. 3(a) and (b), whereas Fig. 4 is depicting the band of circles in black for further processing. Let us assume pupil center as origin of coordinate axes in the image. In lower left and lower right quadrants, a sequence of different one-dimensional signals (radially outwards) is used to pick the boundary pixels coordinates which has significant gradient. Mahalanobis distance [20] is determined from these points to the center of the pupil by using the following formula:

$$\text{Dist} = \sqrt{(x-c)^t \Sigma^{-1} (x-c)},$$

where $\Sigma$ is the covariance matrix and is defined as follows:

$$\Sigma = \int (x-c)(x-c)^t p(x)\,\mathrm{d}x,$$

where $x$ are boundary points and $c$ is the coordinate of center of pupil and $p(x)$ is the probability of point $x$. Maximum number of points with same Mahalanobis distance in a band of eight pixels are used as an adapted threshold to select the points on iris. This threshold is reckoned on the fact that iris and pupil centers are near to each other and selected points are passing through a circle; therefore, remaining (noisy) points are deleted. Parameters of iris circle $A$, $B$ and $C$ are calculated from the selected points using the equation:

$$x^2 + y^2 + Ax + By + C = 0.$$

Center of the iris is $(-A/2, -B/2)$ and radius of iris is $r = \frac{1}{2}\sqrt{A^2 + B^2 - 4C}$. Circular localization of iris is shown in Fig. 5 along with the centers of pupil and iris. This method is effectively applied to both datasets.

### 3.4. Detection of upper and lower eyelids

Iris is bounded in two circles iris/pupil boundary circle and iris/sclera boundary circle, the region of interest is now reduced within iris/sclera boundary. To find the upper eyelid, upper half segment of the image from pupil center is used which lies between the left and right iris boundaries. A virtual parabola ($y^2 = -4ax$) near pupil upper boundary is drawn which passes through three nonlinear points as

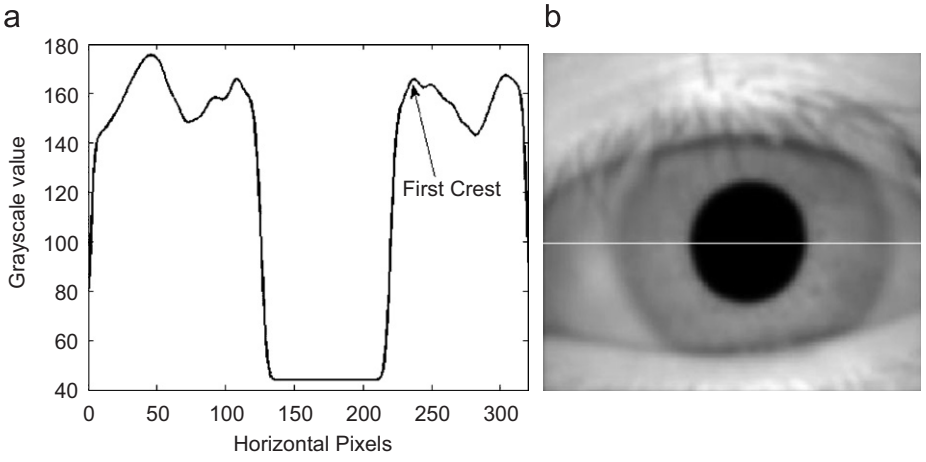


Fig. 3. (a) The horizontal plot of the line passing through pupil center of filtered image (b).

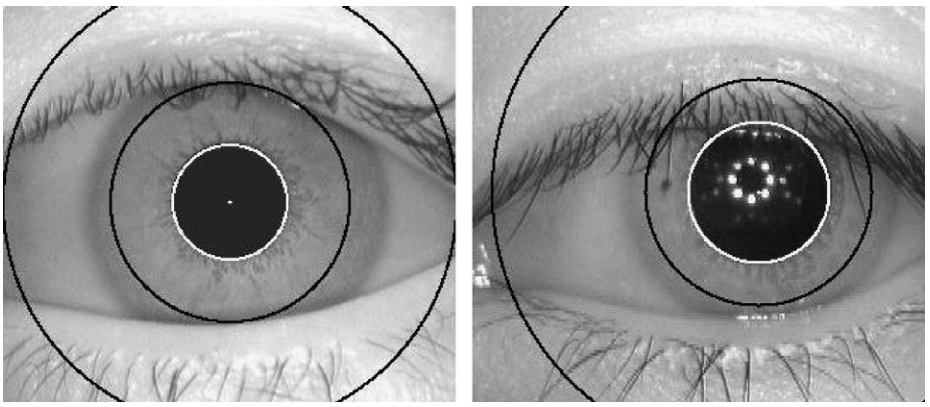

Fig. 4. Band of black circles for finding iris/sclera boundary concentric with white iris/pupil boundary.

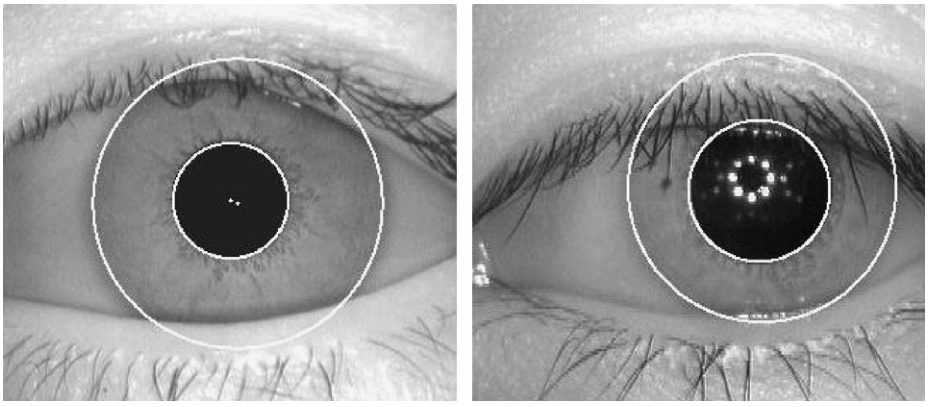

Fig. 5. Localized irises with two circles and their centers.

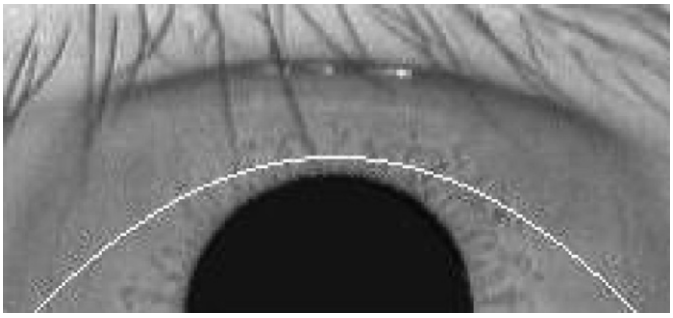

Fig. 6. Virtual parabola for upper eyelid detection.

shown in Fig. 6. Two points are near the left and right iris boundary, and one is three pixels above the pupil boundary in vertical line of pupil center. This virtual parabola makes the processing fast. One-dimensional signals starting from first row of region of interest going vertically downwards till virtual parabola are picked and are smoothed by applying moving average filter of five taps. Maximum three points on each signal are selected for further processing, based on a specific threshold value. If the selected points are not in the region of interest and less than a significant number then it is assumed that iris is not occluded by the eyelid. Among these points, exact eyelid points are selected using following criterions:

(a) $P(x, y) < 120$
The intensity value of image $P(x, y)$ at the point $(x, y)$ must be less than 120, as eyelid is darker part of the image so it has values in the range from 0 to 119.

(b) $P(x, y) \approx \{P(x-1, y-1)$ or $P(x-1, y)$ or $P(x-1, y-1)\}$
Any of the left three neighboring points (upper left, immediate left or lower left) should has almost same intensity value as of the point under consideration.

(c) $P(x, y) \approx \{P(x+1, y-1)$ or $P(x+1, y)$ or $P(x+1, y+1)\}$
Any of the right three neighboring points (upper right, immediate right or lower right) should has almost same intensity value as of the point under consideration.

If a point satisfies all criterions, then it will be a candidate point for parabola. In this way, points which are not on eyelid boundary are deleted and the effect of eyelashes in finding upper eyelid is minimized. Afterwards, a parabola is fitted recursively passing through the remaining points using least square curve fit method which is exactly the upper eyelid.

Lower eyelid is localized almost in the similar fashion. Only the following minor differences are: the lower half segment of the image within iris outer boundary is used. Third point for virtual parabola $y^2 = 4ax$ is three pixels below the pupil boundary and one-dimensional signals are picked in upward direction instead of downward. After this course of action, iris in the image is completely localized by two circles with different centers and two parabolas.

### 3.5. Eyelash removal

The final redundancy left in iris image is presence of eyelashes (which may contribute in false pattern extraction). In the first part of eyelash removal, the histogram of the localized iris is taken. As eyelashes are of low intensity values, therefore, initial part of the histogram reflects the presence of eyelashes. If the number of pixels present in initial part of histogram are within a specified threshold value then the eyelash removal is carried out otherwise it is considered that localized iris is free from eyelashes. Once presence of eyelashes in localized iris image is verified, then image is passed through a high pass filter whose cut off frequency is defined by the maximum intensity value inside the initial part of the histogram. The resultant image is the completely localized iris image free from all noises (i.e. eyelids, pupil, sclera, etc.).

## 4. Experimental results

The proposed algorithm is implemented in Matlab 7.0 on a computer with 1.8 GHz processor and 512 MB RAM. There is no common iris database available for comparison, the CASIA Iris Databases Ver 1.0 and Ver 3.0 are used [19]. CASIA Ver 1.0 contains 756 iris images

($320 \times 280$ pixels resolution) of 108 different people and each has seven images which are captured in two different sessions of 1 month difference. Three images were acquired in first session and four in second session. CASIA Ver 3.0 contains three subsets from which CASIA-IrisV3-Interval is used for experiments having 2655 images ($320 \times 280$ pixels resolution) of 249 people and image of each (left and right) eye is captured at most 10 times. The results observed by eyes of proposed algorithm on the 756 and 2655 images of the dataset are given in the succeeding paragraphs.

### 4.1. Experiment set 1

In first set of experiments, results are collected on iris localization and accuracy of results is compared with respect to ideal exact iris localization. Iris is bounded by two circles in each image and centers of the circles with white dot can also be seen. Iris and pupil center are different in majority of images. The results (CASIA Ver 1.0) shown in Table 1 reflect the accuracy of proposed algorithm is up to 99.6% and the mean processing time is 0.33 s per image whereas minimum and maximum time used are 0.24 and 0.41 s, respectively. Other results (CASIA Ver 3.0) are 99.07% with mean time elapsed is 0.47 s and optimal readings are 1.21 and 0.37 s. Main reason for larger time consumption in CASIA Ver 3.0 is due to the presence of bright spots inside the pupil.

Table 1
Accuracy and time for iris segmentation

| | Accuracy (%) | Time (s) | | |
|---|---|---|---|---|
| | | Mean | Minimum | Maximum |
| CASIA Ver 1.0 | 99.6 | 0.33 | 0.24 | 0.41 |
| CASIA Ver 3.0 | 99.07 | 0.47 | 0.37 | 1.21 |

Table 2
Accuracy and time for upper eyelid

| | Accuracy (%) | Time (s) | | |
|---|---|---|---|---|
| | | Mean | Minimum | Maximum |
| CASIA Ver 1.0 | 98.91 | 0.36 | 0.30 | 0.39 |
| CASIA Ver 3.0 | 90.02 | 0.31 | 0.28 | 0.33 |

### 4.2. Experiment set 2

In this set of experiments, the upper eyelid segmentation is performed through proposed algorithm and results are shown in Table 2. The result of upper and lower eyelids segmentation is shown in Fig. 7 for different iris images, upper row in the figure represents images from CASIA Ver 1.0 and lower row describes CASIA Ver 3.0 images. If eyelids are occurred in iris image then one or two parabolas are drawn by the proposed method otherwise eyelid is not detected by the system. In CASIA Ver 1.0, the accuracy of upper eyelid localization is achieved up to 98.91% with computation mean time of 0.36 s per image. The accuracy rate of CASIA Ver 3.0 is 90.02% with average time of 0.31 s per image.

### 4.3. Experiment set 3

In this set of experiments, the lower eyelids segmentation is performed through proposed algorithm. Lower eyelid segmentation is also shown in Fig. 7, and the results are tabulated in Table 3. The success rate of lower eyelid localization is attained up to 97.8% in CASIA Ver 1.0 with mean processing of 0.4 s, maximum and minimum time utilized are 0.42 and 0.37 s, respectively. In CASIA Ver 3.0, correct lower eyelid detection rate is 91.9%. In this process, average time consumed is 0.3 s per image, whereas extreme time readings are 0.27 and 0.35 s.

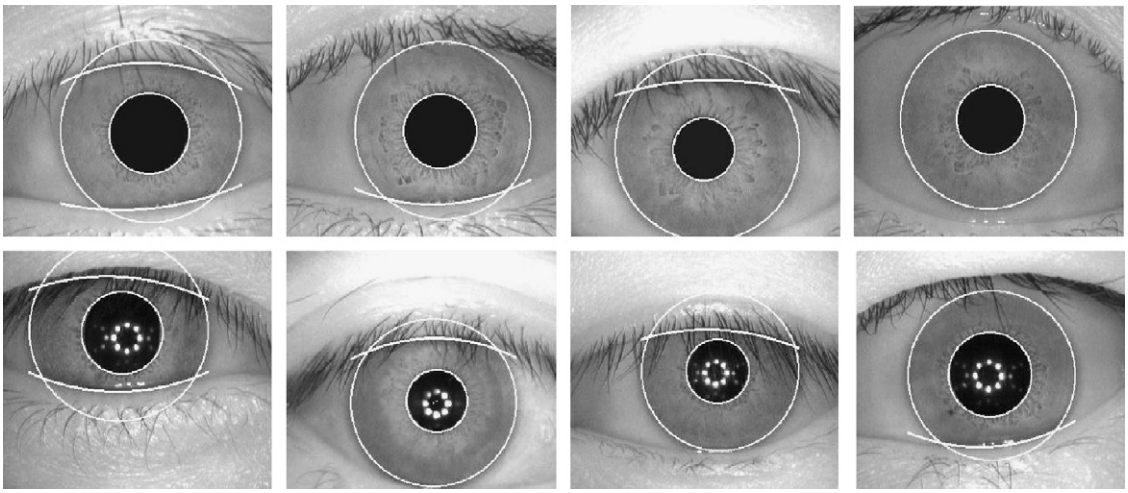

Fig. 7. Completely localized irises; upper row is for CASIA Ver 1.0 and lower row is for CASIA Ver 3.0.

Table 3
Accuracy and time for lower eyelid

| | Accuracy (%) | Time (s) | | |
|---|---|---|---|---|
| | | Mean | Minimum | Maximum |
| CASIA Ver 1.0 | 97.8 | 0.40 | 0.37 | 0.42 |
| CASIA Ver 3.0 | 91.9 | 0.30 | 0.27 | 0.35 |

Table 4
Comparison with other methods

| Method | Accuracy (%) | Time (s) | | |
|---|---|---|---|---|
| | | Mean | Minimum | Maximum |
| Daugman [4] | 98.6 | 6.56 | 6.23 | 6.99 |
| Wildes [7] | 99.9 | 8.28 | 6.34 | 12.54 |
| Cui et al. [14] | 99.3 | 0.24 | 0.18 | 0.33 |
| Shen et al. [21] | Not mentioned | 3.8 | – | – |
| Proposed | 99.6 | 0.33 | 0.24 | 0.41 |

Table 5
Comparison with other methods

| Method | Upper eyelid | | Lower eyelid | |
|---|---|---|---|---|
| Daugman [4] | N/A | | N/A | |
| Wildes [7] | N/A | | N/A | |
| Shen et al. [21] | N/A | | N/A | |
| | Accuracy (%) | Mean time (s) | Accuracy (%) | Mean time (s) |
| Cui et al. [14] | 97.35 | 0.18 | 93.39 | 0.77 |
| Proposed | 98.91 | 0.36 | 97.80 | 0.40 |

## 5. Discussions

Results of correct iris localization on iris databases CASIA Ver 1.0 and Ver 3.0 are 99.6% and 99.07%, respectively. CASIA Ver 3.0 has more percentage of blurred images as compared to Ver 1.0. Therefore, overall results are better in CASIA Ver 1.0, particularly in the process of detection of upper and lower eyelids. Tables 1–3 contain results of the proposed algorithm for iris boundaries, upper and lower eyelid localization, respectively, and their comparison with existing techniques is shown in Tables 4 and 5. These results reflect that the accuracy of proposed algorithm is up to 99.6%.

It is obvious from the figures given in Table 4 that proposed system has higher accuracy than Daugman and Cui's iris localization method [4,14]. Average time used by the proposed system is very low as compared to Daugman and Wildes systems. Maximum time spent to localize iris is 0.41 s which is almost 30 times less than Wildes and 17 times less than Daugman, whereas it takes only 0.08 s more than Cui's method. It is approximately 26 times faster than Daugman and Wildes while comparing minimum time usage. It is also observed that accuracy of the proposed system is slightly less (i.e. 0.3%) than that of Wildes method [7] but Wildes method is very time consuming. Average time used by his system is 8.28 s per image. On the other hand, proposed system is utilizing only 0.33 s which is 25 times faster than that of Wildes. Cui's method takes 0.09 s less but its accuracy is also less than the proposed method.

Comparison of upper and lower eyelid segmentation is given in Table 5. It is clear from the table that proposed method is better than Cui both in localization of upper and lower eyelids. Daugman and Wildes did not perform eyelid segmentation. Accuracy of proposed eyelid localization method is better than Cui's by 1.06% and 4.1% for upper and lower eyelid, respectively. Mean time consumption on each image is 0.36 s in upper eyelid segmentation and is 0.4 s in lower eyelid segmentation, while it takes 0.19 s less than other method in obtaining both eyelids. However, the method proposed in this paper outperforms in the process of iris localization.

## 6. Conclusions

Iris localization is the most important step in iris recognition systems. In this research work, a novel and fast method of complete iris localization is proposed based on intensity value analysis of gray scale eye images. Iris is localized by first finding the boundary between pupil and iris using two different methods for two databases. The boundary between iris and sclera is then obtained by finding points of maximum gradient in radially outwards different directions. Redundant points are discarded using Mahalanobis distance. The domain for different directions is left and right lower half quadrants when pupil center is at the origin of the axes. Eyelids are detected by getting parabolas using points satisfying different criterions and then eyelashes are removed using adaptive high pass filter. Experimental results show the efficiency of the proposed method.

## Acknowledgments

The authors wish to thank Chinese Academy of Sciences—Institute of Automation for providing the iris database and Mr. Muhammad Abdul Samad and Mr. Saqib Masood for their helpful suggestions and fruitful discussions. The shared CASIA Iris Databases are available on the web [19].

## References

[1] Ali JMH, Hassanien AE. An iris recognition system to enhance e-security environment based on wavelet theory. Adv Model Opt 2003;5(2):93–104.
[2] Basit A, Javed MY, Anjum MA. Efficient iris recognition method for human identification. Enformatika 2005;1:24–6.

[3] Basit A, Javed MY. A fast and robust iris localization method. In: Proceedings of IADIS international conference applied computing; 2006. p. 557–60.
[4] Daugman JG. High confidence visual recognition of persons by a test of statistical independence. IEEE Trans Pattern Anal Mach Intell 1993;5(11):1148–61.
[5] Daugman J. The importance of being random: statistical principles of iris recognition. Pattern Recog 2003;36:279–91.
[6] Wildes R, Asmuth J, et al. A machine vision system for iris recognition. Mach Vision Appl 1996;9:1–8.
[7] Wildes R. Iris recognition: an emerging biometric technology. Proc IEEE 1997;85(9):1348–63.
[8] Ma L, Tan T, Wang Y. Efficient iris recognition by characterizing key local variations. IEEE Trans Image Process 2004;13(6):739–50.
[9] Kronfeld P. Groos anatomy and embryology of the eye. In: Davson H, editor. The eye. London: Academic Press; 1962.
[10] Adler F. Physiology of the eye: clinical application. 4th ed. London: The C.V. Mosby Company; 1965.
[11] Liam LW, Chekma A, Fan LC, Dargham JA. Iris recognition using self organizing neural networks. In: 2002 Student conference on research and development proceedings, Malaysia; 2002. p. 169–72.
[12] Hallinan PW. Recognizing human eyes. Geom Meth Comput Vision 1991;1570:214–26.
[13] Snell RS, Lemp MA. Clinical anatomy of the eye. 2nd revised ed. Blackwell Science Inc.; 1998.
[14] Cui J, Wang Y, Tan T, Ma L, Sun Z. A fast and robust iris localization method based on texture segmentation. SPIE Def Secur Symp 2004;5404:401–8.
[15] Ma L, Wang Y, Tan T. Iris recognition based multi-channel Gabor filtering. In: The fifth Asian conference on computer vision, 23–25 January 2002.
[16] Kim J, Cho S, Choi J. Iris recognition using wavelet features. J VLSI Signal Process 2004;38:147–56.
[17] Bernogger S, Yin L, Basu A, Pinz A. Eye tracking and animation for MPEG-4 coding. In: Proceedings of 14th ICPR, vol. 2 1998. p. 1281–4.
[18] Xie X, Sudhakar R, Zhuang H. Real time eye feature tracking from a video image sequence using Kalman filter. IEEE Trans Syst Man Cybern 1995;25(12):1568–77.
[19] Chinese Academy of Sciences—Institute of Automation (CASIA) Iris database; 〈http://www.sinobiometrics.com〉.
[20] Duda RO, Hart PE, Stork DG. Pattern classification. 2nd ed. Wiley-Interscience Publication; 2001.
[21] Shen YZ, Zhang MJ, Yue JW, Ye HM. A new iris locating algorithm. In: Proceedings of the international conference on artificial reality and telexistence—workshops (ICAT'06); 2006. p. 438–41.